Supporting Information

Analysis of Extracellular Vesicles Using Coffee- ring

Hwapyeong Jeong,[1] Chungmin Han,[1] Siwoo Cho,[1]Yogesh Gianchandani,[3*] and Jaesung Park[1,2,3 *]

[1]*Mechanical Engineering, POSTECH, Republic of Korea*

[2]*School of Interdisciplinary Bioscience and Bioengineering, POSTECH, Republic of Korea*

[3] *Center for Wireless Integrated MicroSensing and Systems, University of Michigan, Ann Arbor, U.S.A.*

** co-corresponding authors*

Figure S1. Contact angle of evaporating droplet (a) Contact angle θ of the droplet on a glass surface during evaporation. τ is the characteristic time. (b) Diameter of the droplet is constant, and θ decreased until τ ~0.4. Afterwards, the edge of the droplet receded.

Figure S2. Spatial resolution of system. (a) Example of ideal Gaussian intensity profile of two sizes of beads (p is position in pixel and h is full-width-half-maximum of an individual mode); (b) virtual band (red line) which is overlapped with another peak.

Figure S3. Confirmation of EVs. (a) Western blot image of EVs from WM266-4 and MCF-7. TEM images of (b) natural EVs, anti-CD9 stained EVs, anti-CD63 stained EVs, and anti-CD81 stained EVs from MCF-7. All images are at the same magnification. (c) DLS data of antibody-stained EVs from MCF-7. The major peaks of the EVs' sizes were not changed. (d) Low magnification SEM image of dried ring pattern of EVs. The size of EVs continuously increases from contact line to the center of the droplet.

Figure S4. Various effects of coffee-ring formation. (a) Fluorescence images of dried separation patterns of EVs from MCF-7 without temperature gradient. Green: CD9-stained EVs, red: CD63-stained EVs. (b) Fluorescence images of EVs dried separation patterns of antibody stained EVs (green: CD9-stained EVs, red: CD63-stained EVs) on different antibody-coated glass slides. (c) Fluorescence image of dried pattern of antibody mixture (anti-CD9: green and anti-CD63: red) in DI water. Antibodies (anti-CD9 and anti-CD63) were not distinguishable by size. The ring pattern separation of EVs was not affected by unbound antibodies.

Figure S5. Dried patterns separation of EVs of WM 266-4 (a, b, and c) Fluorescence images of dried pattern separation of EVs of WM 266-4 with a temperature gradient of 2 °C/mm. (a) Red: CD63-stained EVs; green: CD9-stained EVs. CD9-stained EVs are smaller than CD63-stained EVs because smaller particles are deposited outside of the ring pattern. (b) Red: CD63-stained EVs; green: CD81-stained

EVs. CD81-dominated EVs are smaller than CD63-dominated EVs. (c) Red: CD81-stained EV; green: CD9-stained EVs. CD9-stained EVs and CD81-stained EVs are not distinguishable by size. Graphs: RGB profiles of ring patterns along the white arrow. Each image is split into green and red channels. (d) Fluorescence images of dried separation patterns of EVs from WM 266-4. SEM image of dried patterns of EV. (e) Inner edges of ring patterns and (f) outer edge of ring patterns of EVs pattern from WM 266-4. (g) In the pattern from WM 266-4, the average size of CD63-high expressed EVs was higher than CD9- or CD81-high expressed EVs. The total number of counted vesicles were n > 160 for all cases.

1. Material and method

EV harvesting condition

Cells (MCF-7, WM 266-4) were cultured using minimum essential media (MEM, GIBCO) supplemented with 10% FBS and 1% penicillin/streptomycin. When cells reached about 90% confluency, culture media was changed to EV preparation medium, which is composed of MEM supplemented with 10% EV-depleted FBS and 1% penicillin/streptomycin. The cells were further cultured for 24 h. Viability of cells was measured by the trypan blue exclusion test, and higher than 95% after culture. Cell-cultured media were centrifuged at 500 x g for 5 min to remove the remaining cells, and then 3000 x g centrifugation was applied for 20 min to remove dead cells and cellular debris. The supernatants were then ultracentrifuged at 100,000 x g for 2 h to isolate EVs. We obtained about 3 x 10^{10} EVs from two million WM 266-3 cells and about 2 x 10^{10} EVs from two million MCF-7 cells. The pellets of EVs were resuspended in PBS and ultracentrifuged again with the same condition.

Antibody staining conditions

Concentration of EVs isolated using double-pelleting methods was adjusted to 500 μg/mL and mixed with tetraspanin antibodies that were crossed linked with various fluorescent dyes. In our system, we used 1 to 100 dilutions for all antibodies (1:100, ab18241, ab77227, ab79559, ab133579 and ab47052, AbCam) and incubated antibody-EV mixtures at 4°C overnight for staining. After incubation, the samples were ultracentrifuged twice at 100,000 x g for 2 h to remove unbound antibodies. A control group was prepared following the same procedure using EV-free PBSs and tested for the effect of antibodies on the coffee-ring separation.

Buffer exchange condition (PBS to distilled water)

To change the buffer of EVs from PBS to distilled water (DW) without abruptly disrupting their morphology, we gradually added DW to the EVs in PBS solution. In detail, 250 μL DW was added to 750 μL EVs in PBS solution to make 25% DW solution and incubated for 10 min at room temperature. 500 μL DW was then further added to the 25% DW solution to make 50% DW solution, and incubated for 10 min at room temperature. Lastly, 1.5 mL DW was added again to make 75% DW solution and ultracentrifuged at 100,000 x g for 2 h to pellet EVs. The EV pellets were then resuspended with DW. The number of particles was 4.7×10^7 particles/1μl in the case of MCF-7 EVs and 7.5×10^7 particles/1μL in the case of WM266-4. Using all of the EVs from one batch, we can generate about four hundred droplets at a protein concentration of ~100 μg/mL (in other words, 4 droplets per 1 mL initial cell-cultured media).

Polystyrene particle preparation

All particles used in the chromatography experiments were suspended in deionized water to prevent crystal formation from trace quantities of salt that would otherwise remain after evaporation. Fluorescent polystyrene spheres (density 1.05 g/cm^3) of D = 1 μm, 500 nm, 100 nm, and 22 nm were suspended in deionized water at an initial volume fraction ~0.003%.

Western blotting

Each sample (5 μg) was separated using SDS-PAGE (12% resolving gel, 120 V, 90 min) and transferred to a PVDF membrane at 390 mA and 4 °C for 2 h. After transferring, the membrane was blocked with 3% non-fat dry milk (Santa Cruz) in Tris-buffered saline (TBS) for 1 h at RT. The blocked membrane was incubated with anti-beta-actin (1:1000, sc-81178, Santa Cruz), anti-CD9 (1:1000, sc-9148, Santa Cruz), anti-CD63 (1:1000, sc-15363, Santa Cruz), anti-CD81 (1:2500, ab93485, AbCam) primary antibodies in blocking solution at 4 °C overnight, and washed with TBST (0.05% tween 20 in TBS). Finally, horseradish-peroxidase-conjugated anti-mouse for beta-actin, and anti-rabbit for CD9, CD63, and CD81 secondary antibody (1:5000, sc-2004, Santa Cruz) were

attached at RT for 1 h, and washed with TBST. The bands were developed using chemiluminescent substrate (Thermo Scientific).

Transmission electron microscopy

Concentration of EVs isolated by double-pelleting methods was adjusted to 500 μg/mL, and the sample of EVs was diluted to concentration of 5 μg/mL in PBS for measurement. To visualize the morphology of the EVs, transmission electron microscopy (TEM) was performed. 5 μL of each sample was deposited on a formavar carbon film (FCF300-cu, Electron Microscopy Science), and then mixed with 7 μL of 2% uranyl acetate for 10 s for staining. Samples were air-dried for 30 min, and then imaged at 60-kV acceleration voltage on a Jeol transmission electron microscope (JEM-1011).

Scanning electron microscopy

To visualize the morphology and size of the EVs, scanning electron microscopy (SEM) was performed. 1 μL of each droplet was placed on the glass surface and dried out under the condition of temperature gradient of $\Delta T/\Delta z = 2$ °C/mm and humidity ~55%. After drying, Pt was coated on glass using a metal sputter, and then imaged at 5-kV acceleration voltage on a Jeol scanning electron microscope (JEOL JSM-7401F).

Dynamic laser scattering

The size distributions of normal EVs and isolated EVs were measured using a dynamic laser scattering (DLS) instrument (Zetasizer 3000HSA, Malvern Instruments). The polydispersity index (PdI) was approximately 0.3

Coffee-ring formation

The prepared EVs and fluorescence polystyrene particle samples were placed on commercial slide glass (Matsunimi) that had been cleaned using acetone and isopropyl alcohol. After cleaning, the

contact angle θ of glass with water/air was ~10°. The glass was set inside of the environmental chamber, and then a 1-μL sample was placed on the glass surface. The protein concentration of all samples was 100 μg/mL by Bradford assay. All patterns were observed under an inverted fluorescence microscope (IX70, Olympus).

2. Contact angle of evaporating droplet

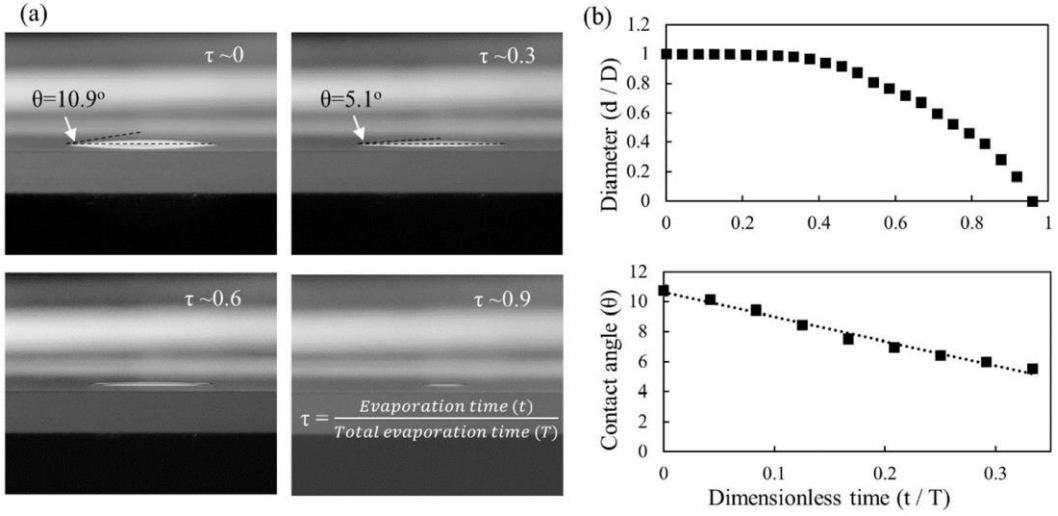

Figure S1. Contact angle of evaporating droplet (a) Contact angle θ of the droplet on a glass surface during evaporation. τ is the characteristic time. (b) Diameter of the droplet is constant, and θ decreased until τ ~0.4. Afterwards, the edge of the droplet receded.

3. Spatial resolution of method

To define the resolution of our system more precisely, we calculated full width at half maximum value, which is also known as spatial resolution. In addition, we compared the resolution of our system with size exclusion chromatography.

From the image of the separated band of a standard size bead, the intensity profile can be obtained along the direction of separation occurrence (Supplementary Fig. 2a). If there is a band of particle having a size close to bead 1, the band is partially overlapped (Supplementary Figure. 2b). As is

commonly known in the definition of spatial resolution, when two peaks of band are overlapped where half maximum of each band matches, it is considered that the bands have reached the resolution limit.

In order to find size separation resolution R_s from the spatial limit, the domain of the intensity profile should be transformed from pixel to diameter space. Assuming that the band position has a linear relationship to particle size, intensity at a certain position is expressed as p_2-p_1=k(d_2-d_1), where d is the diameter of the particle and k is (p_2-p_1)/(d_2-d_1). Therefore, R_s is

$$R_s = 2h\left(\frac{d_2 - d_1}{p_2 - p_1}\right).$$

R_s describes the minimum difference of particle sizes where the bands that the particles formed are distinguishable from each other. In this system with temperature gradient at $\Delta T/\Delta z$ = 2 °C/mm, the resolution is 48 nm.

To estimate the separation performance of general chromatography, the theoretical plate number is defined as

$$N_{chromato} = 5.545\left(\frac{t_R}{w_b}\right)^2$$

where t_R is the retention time (elapsed time for that band to appear); and w_b is the full-width-half-maximum in temporal dimension. However, because Marangoni separation does not occur along time but on a plane, the conventional definition of plate number in chromatography into compatible form for the coffee-ring method should be modified to

$$N_m = 5.545\left(\frac{r}{2h}\right)^2$$

where r is retention distance; and 2h is full-width-half-maximum. In the coffee-ring method, the particle is stacked from the outer edge of the droplet, and the edge is not clearly shown. Consequently, the arc made by the smallest bead fraction is regarded as the edge and origin of the coordination, and retention distance r become r=p_2-p_1.

$$N_m = 5.545\left(\frac{p_1 - p_2}{2h}\right)^2.$$

Comparing column efficiency with plate number between the coffee-ring method and SEC, plate number of the coffee-ring method was about 400 N larger than that SEC media, Sepharose CL2, about

186 N. In this system, two bands composed of two different sizes can be resolved down to a size difference of 48 nm.

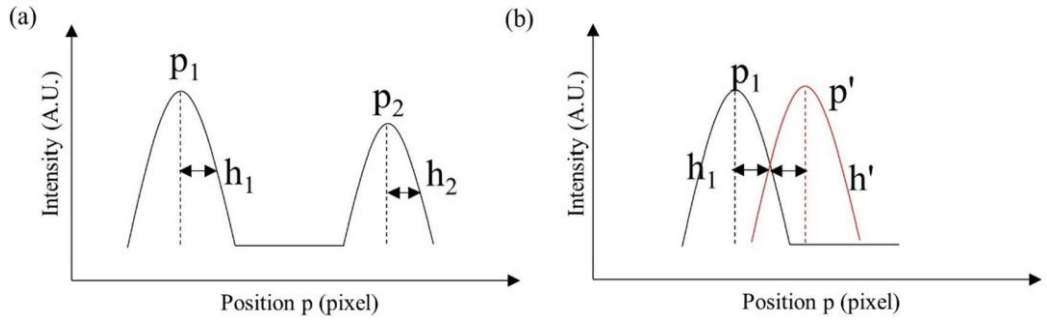

Figure S2. Spatial resolution of system. (a) Example of ideal Gaussian intensity profile of two sizes of beads (p is position in pixel and h is full-width-half-maximum of an individual mode); (b) virtual band (red line) which is overlapped with another peak.

4. Confirmation of EVs

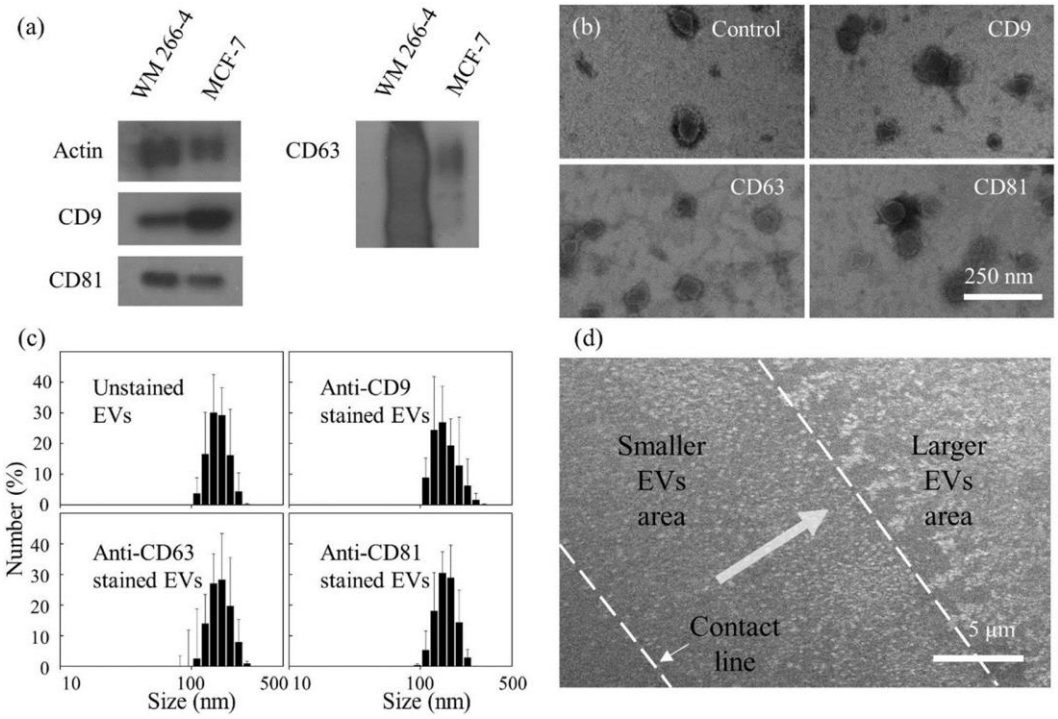

Figure S3. Confirmation of EVs. (a) Western blot image of EVs from WM266-4 and MCF-7. TEM images of (b) natural EVs, anti-CD9 stained EVs, anti-CD63 stained EVs, and anti-CD81 stained EVs from MCF-7. All images are at the same magnification. (c) DLS data of antibody-stained EVs from MCF-7. The major peaks of the EVs' sizes were not changed. (d) Low magnification SEM image of dried ring pattern of EVs. The size of EVs continuously increases from contact line to the center of the droplet.

5. Various ring patterns of EVs

To confirm the impact of antibodies, EVs were post-stained with antibodies (CD9, CD63) after the coffee-ring formation. The post-stained EVs ring pattern showed the same result as the previous result. For the same purpose, without EVs, only anti-CD9 and anti-CD63 were mixed, and the mixture was dried under the same condition as the coffee-ring formation. The ring patterns of unbounded antibodies were not distinguishable, indicating that antibodies do not affect the ring pattern.

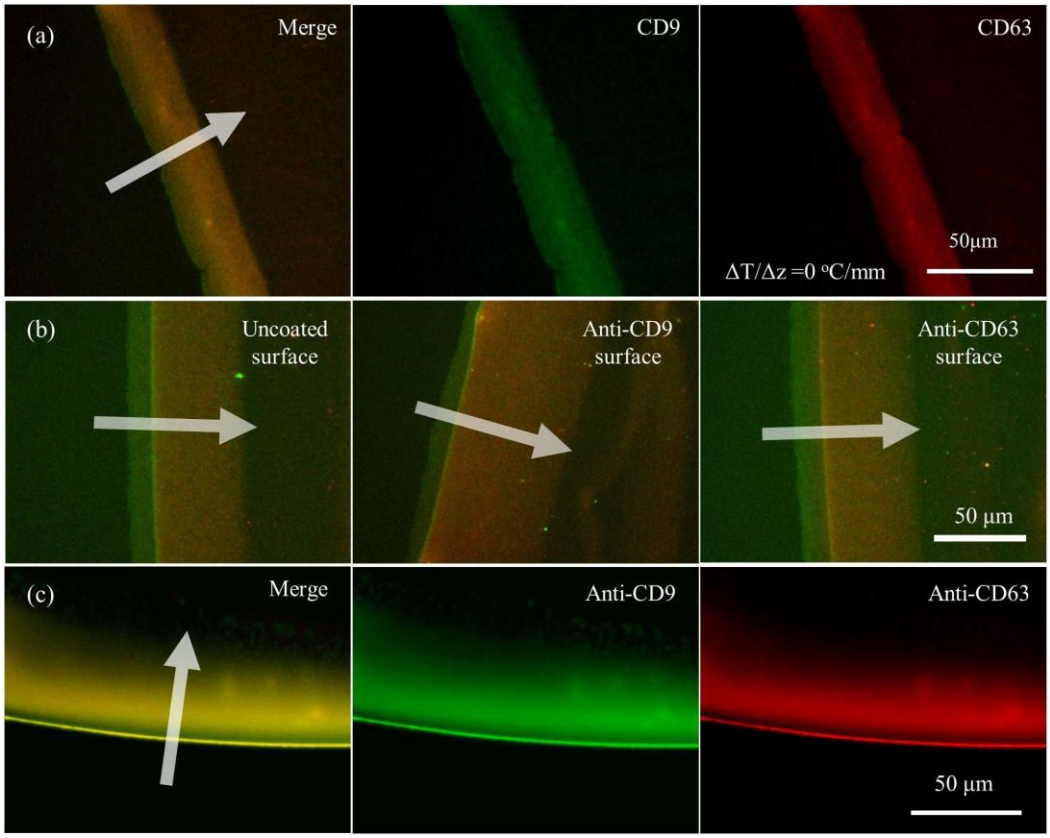

Figure S4. Various effects of coffee-ring formation. (a) Fluorescence images of dried separation patterns of EVs from MCF-7 without temperature gradient. Green: CD9-stained EVs, red: CD63-stained EVs. (b) Fluorescence images of EVs dried separation patterns of antibody stained EVs (green: CD9-stained EVs, red: CD63-stained EVs) on different antibody-coated glass slides. (c) Fluorescence image of dried pattern of antibody mixture (anti-CD9: green and anti-CD63: red) in DI water. Antibodies (anti-CD9 and anti-CD63) were not distinguishable by size. The ring pattern separation of EVs was not affected by unbound antibodies.

6. Coffee-ring pattern of EVs from WM 266-4

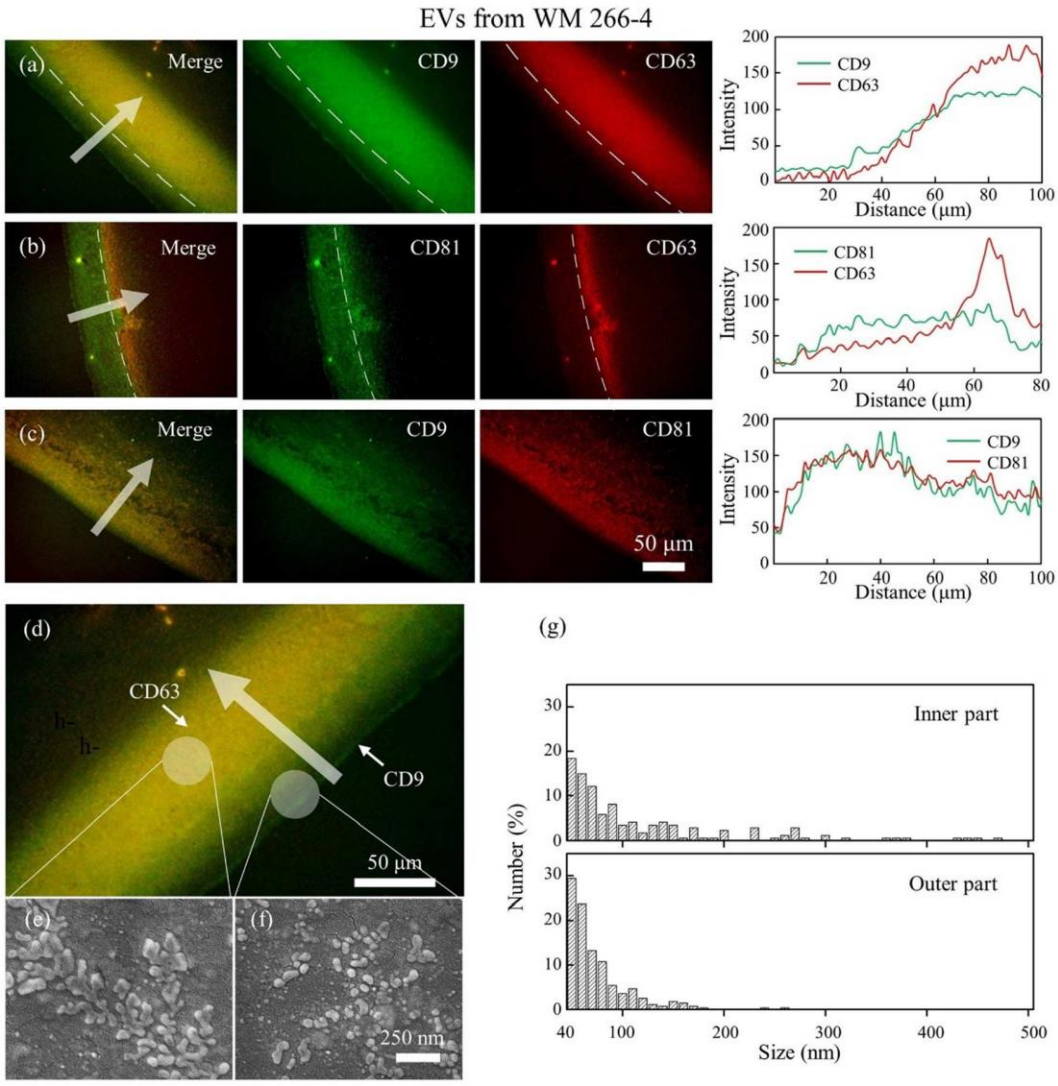

Figure S5. Dried patterns separation of EVs of WM 266-4 (a, b, and c) Fluorescence images of dried pattern separation of EVs of WM 266-4 with a temperature gradient of 2 °C/mm. (a) Red: CD63-stained EVs; green: CD9-stained EVs. CD9-stained EVs are smaller than CD63-stained EVs because smaller particles are deposited outside of the ring pattern. (b) Red: CD63-stained EVs; green: CD81-stained EVs. CD81-dominated EVs are smaller than CD63-dominated EVs. (c) Red: CD81-stained EV; green: CD9-stained EVs. CD9-stained EVs and CD81-stained EVs are not distinguishable by size. Graphs: RGB profiles of ring patterns along the white arrow. Each image is split into green and red channels. (d) Fluorescence images of dried separation patterns of EVs from WM 266-4. SEM image of dried patterns of EV. (e) Inner edges of ring patterns and (f) outer edge of ring patterns of EVs pattern from WM 266-4. (g) In the pattern from WM 266-4, the average size of CD63-high expressed EVs was higher than CD9- or CD81-high expressed EVs. The total number of counted vesicles were n > 160 for all cases.